AJNR

Is the Subthalamic Nucleus Hypointense on T2-Weighted Images? A Correlation Study Using MR Imaging and Stereotactic Atlas Data

Didier Dormont, Kenneth G. Ricciardi, Dominique Tandé, Karine Parain, Carole Menuel, Damien Galanaud, Soledad Navarro, Philippe Cornu, Yves Agid and Jérôme Yelnik

AJNR Am J Neuroradiol 2004, 25 (9) 1516-1523
http://www.ajnr.org/content/25/9/1516

AJNR Am J Neuroradiol 25:1516–1523, October 2004

Is the Subthalamic Nucleus Hypointense on T2-Weighted Images? A Correlation Study Using MR Imaging and Stereotactic Atlas Data

Didier Dormont, Kenneth G. Ricciardi, Dominique Tandé, Karine Parain, Carole Menuel, Damien Galanaud, Soledad Navarro, Philippe Cornu, Yves Agid, and Jérôme Yelnik

BACKGROUND AND PURPOSE: **Although the subthalamic nucleus is the most frequently used target for surgical treatment of Parkinson's disease, the criteria on which it can be identified on T2-weighted images have never been clearly defined. This study was conducted to characterize the precise anatomic distribution of T2-weighted hyposignal in the subthalamic region and to correlate this hyposignal with iron content in the subthalamic nucleus.**

METHODS: **The T2-weighted MR imaging acquisitions of 15 patients with Parkinson's disease were fused with a digitized version of the Schaltenbrand and Wahren anatomic atlas. The MR signal intensity within the anatomic limits of the subthalamic nucleus was evaluated. An anatomic specimen obtained at autopsy was used to evaluate iron content.**

RESULTS: **In all patients, the subthalamic nucleus was hypointense on both sides in the anterior half of the nucleus. At more posterior levels of the nucleus, hypointensity was less frequently observed (20–80%). Hypointensity was never observed at the most posterior pole. Iron was present in the anteromedial part of the nucleus but absent at the most posterior levels.**

CONCLUSION: **The hypointense signal intensity located lateral to the red nucleus and dorsolateral to the substantia nigra correlates with the presence of iron and corresponds anatomically to the subthalamic nucleus. It can therefore be used as a landmark for electrode implantation in patients with Parkinson's disease. It should, however, be emphasized that although hypointensity was always present in the anterior half of the subthalamic nucleus, the posterior part of the nucleus was not visible in most cases.**

Bilateral electrode implantation at the level of the subthalamic nuclei (STN), plus continuous high frequency stimulation by means of a pacemaker, constitutes a new treatment for advanced Parkinson's disease (1–4). The STN is a biconvex lens-shaped obliquely oriented nucleus located on the dorsomedial surface of the peduncular part of the internal capsule, which, because of its small dimensions and anatomic characteristics, is difficult to localize (5). Furthermore, the STN presents significant interindividual topographic variations in size and shape that make difficult a precise prediction of its localization based only on statistical considerations and stereotactic atlases (6, 7). For this reason, the use of MR imaging has been advocated for the direct targeting of this nucleus (1–3, 6, 8, 9). T2-weighted sequences have been proposed because the region of the STN, located lateral to the red nucleus and dorsolateral to the substantia nigra, appears as hypointense signal intensity and can therefore be easily identified. In addition, hypointensity is generally attributed to iron deposition, and many studies have shown that iron is particularly present at the level of the basal ganglia (10–17). However, the criteria on which this nucleus can be unambiguously identified have never been clearly defined, and identifying the hypointense signal intensity lateral to the red nucleus as the STN has, until now, been purely hypothetical. The present study, conducted to answer these questions, comprised two aspects. First, a computerized version (18) of the Schaltenbrand and Wahren anatomic atlas (19) was registered on T2-weighted acquisitions to characterize the distribution of the hyposignal observed in the subthalamic region in terms of precise anatomic

Received January 2, 2004; accepted January 30.

Supported in part by grant 97506 from Medtronic Limited.

Presented at the 41st Annual Meeting of the American Society of Neuroradiology, Washington, DC, May 2003.

From the Departments of Neuroradiology (D.D., K.G.R., D.G.), UPR 640 CNRS LENA (D.D., C.M.), Neurosurgery (S.N., P.C.), Neurology (Y.A.), and INSERM U289 (D.T., K.P., J.Y.), Pitié-Salpêtrière Hospital, Paris, France.

Address reprint requests to Didier Dormont, Department of Neuroradiology and UPR 640 CNRS LENA, Pitié-Salpêtrière Hospital, 47 bd de l'Hôpital, 75651, Paris, Cedex 13, France.

structures. Second, a study based on a Perls stained specimen was performed to correlate this hyposignal with iron content in the STN with the aim of exploring the cellular basis of this distribution.

Methods

MR Imaging Data

This study is based on the T2-weighted acquisitions of 15 patients (nine women and six men; age range, 38–66 years; mean age, 52.6 years) with advanced Parkinson's disease who underwent bilateral electrode implantation at the level of the STN, based on MR imaging findings obtained under stereotactic conditions the day before the surgical intervention. MR imaging was performed on a 1.5-T unit (Signa system; General Electric Medical Systems, Milwaukee, WI), with an MR-compatible Leksell G stereotactic frame (Elekta, Stockholm, Sweden), using a previously described acquisition protocol (1). This protocol included two coronal T2-weighted spin-echo image acquisitions of interleaved 2-mm sections; the first acquisition passing through the posterior commissure, as determined by a 5-mm median spin-echo sagittal T1-weighted image, and the second acquisition being shifted 1 mm more anteriorly (parameters: 2200/90/2 [TR/TE/NEX]; acquisition time for the two studies, 21 minutes 16 seconds). The field of view was 280 mm (superior–inferior direction) × 210 mm (right–left direction), with a matrix size of 256 × 192. The interleaved technique was used to avoid the signal intensity degradation observed when contiguous sections are acquired by using 2D spin-echo acquisitions. This sequence produced heavily T2-weighted images, which are also highly sensitive to local variations of magnetic susceptibility.

Post-Processing of the Data

For each patient, the two coronal T2-weighted acquisitions were fused by using an Advantage Windows workstation (General Electric, Buc, France) to obtain a single data set of 2-mm images every 1 mm. The images were then reformatted to obtain 2-mm-thick frontal sections, perpendicular to the anterior commissure–posterior commissure line, every 1 mm. The reformatted sections were also positioned strictly perpendicular to the midline sagittal plane to correct for any rotation of the patient's head. For each patient, the 2-mm reformatted images were saved in the tif format and transferred to a personal computer. Digitized coronal sections of the Schaltenbrand and Wahren stereotactic atlas were then fused with the MR imaging series of each patient by using a 3D atlas–MR image registration method (18, 20). The distance between the anterior commissure and posterior commissure landmarks was used to establish a proportional correspondence between the sections of the atlas and the reformatted MR images of each patient. The six coronal sections of the Schaltenbrand and Wahren atlas on which the STN was present were superimposed on the MR images. In the atlas, these sections are referred to as Fa 2.0 (2 mm in front of the midpoint of the anterior commissure–posterior commissure distance), Fp 1.5 (1.5 mm behind the midpoint of the anterior commissure–posterior commissure distance), and Fp 3.0, Fp 4.0, Fp 5.0, and Fp 7.0 from anterior to posterior. When the interhemispheric fissure visible on the MR images was not parallel to the vertical axis present on the digitized atlas sections, a rotation was applied to the former to obtain a perfect match between MR images and atlas sections. Each section of the atlas was scaled to the particular size of each T2-weighted MR image of the brain by applying independent factors along the dorsoventral and mediolateral axes. The left and right part of the atlas section could be moved and deformed independently, so that any difference in the width of the third ventricle could be compensated for without affecting the rest of the positioning process. The same factors were applied for all sections in a given patient. The main landmarks used in each section to obtain correct positioning were the substantia nigra, the red nucleus, the lateral wall of the third ventricle, the floor of the lateral ventricle, and the lateral margins of the thalamus. The images with the fused atlas data were then saved as PowerPoint (Microsoft) files.

Evaluation of MR Signal Intensity inside the Limits of the STN

Two neuroradiologists (D.D. and K.G.R.) independently evaluated the presence of a hypointense signal intensity on the T2-weighted coronal images within the limits of the STN, as defined by fusion with the Schaltenbrand and Wahren atlas. The thalamus, which was present in all the examined sections, was used as an internal reference. Findings on coronal T2-weighted MR images were scored as 1 for isointense, in the absence of significant signal intensity differences between the thalamus and the area corresponding to the STN on the atlas section; 2 for intermediate, in the presence of a mild or medium hypointensity in the area corresponding to the STN compared with that of the thalamus; or 3 for hypointense, in the presence of a prominent decreased signal intensity in the area corresponding to the STN compared with that of the thalamus. Disagreements in scoring between the two neuroradiologists were resolved by consensus.

Histologic Data on an Anatomic Specimen

A brain obtained at autopsy of a donated cadaver was used for this study. Death had resulted from cardiac failure. The patient had no history of neurologic disease, as verified in the clinical chart. The brain was extracted after a postmortem delay of 38 hours. It was separated into two hemispheres, which were left in a 4% paraformaldehyde solution for 2 days. It was then sectioned perpendicularly to the anterior commissure–posterior commissure line into 1.5-cm-thick blocks, which were left in another solution of 4% paraformaldehyde for 2 weeks. Each block was cut into 70-μm-thick sections on a freezing microtome. The sections were rinsed in phosphate-buffered saline for 10 minutes and left in a mixture of 20% methanol and 3% hydrogen peroxide for inhibition of endogenous peroxidases. The sections were then rinsed again and post-fixed in 4% paraformaldehyde for 3 hours. A Perls reaction (21) was performed in a mixture of 4% hypochloric acid and 4% potassium ferrocyanide for 20 minutes. Finally, counterstaining was performed in a solution of neutral red for 6 minutes.

The contours of cerebral structures were traced under microscopic examination on the basis of their cytoarchitectonic characteristics. This was performed on the basis of the counterstaining in the Perls stained sections and also in a series of adjacent sections stained by the Nissl technique. Thus, the 3D consistency of the contours could be verified along an anteroposterior series of successive sections.

Results

Figure 1 shows an example of the fusion of T2-weighted images with the Schaltenbrand and Wahren atlas. The scale correction factor that was applied to the Schaltenbrand and Wahren atlas to match the reformatted T2-weighted images varied from 0.84 to 0.96 in the dorsoventral direction (0.91 ± 0.04 [mean ± SD]) and from 0.92 to 1.08 in the mediolateral direction (0.99 ± 0.05). The distance between the left and right parts of the Schaltenbrand and Wahren atlas sections was 2 mm ± 0.8 at the level of the most posterior section (Fp 7) and 5.1 mm ± 1.4 at the level of the most anterior section (Fa 2). This slight in-

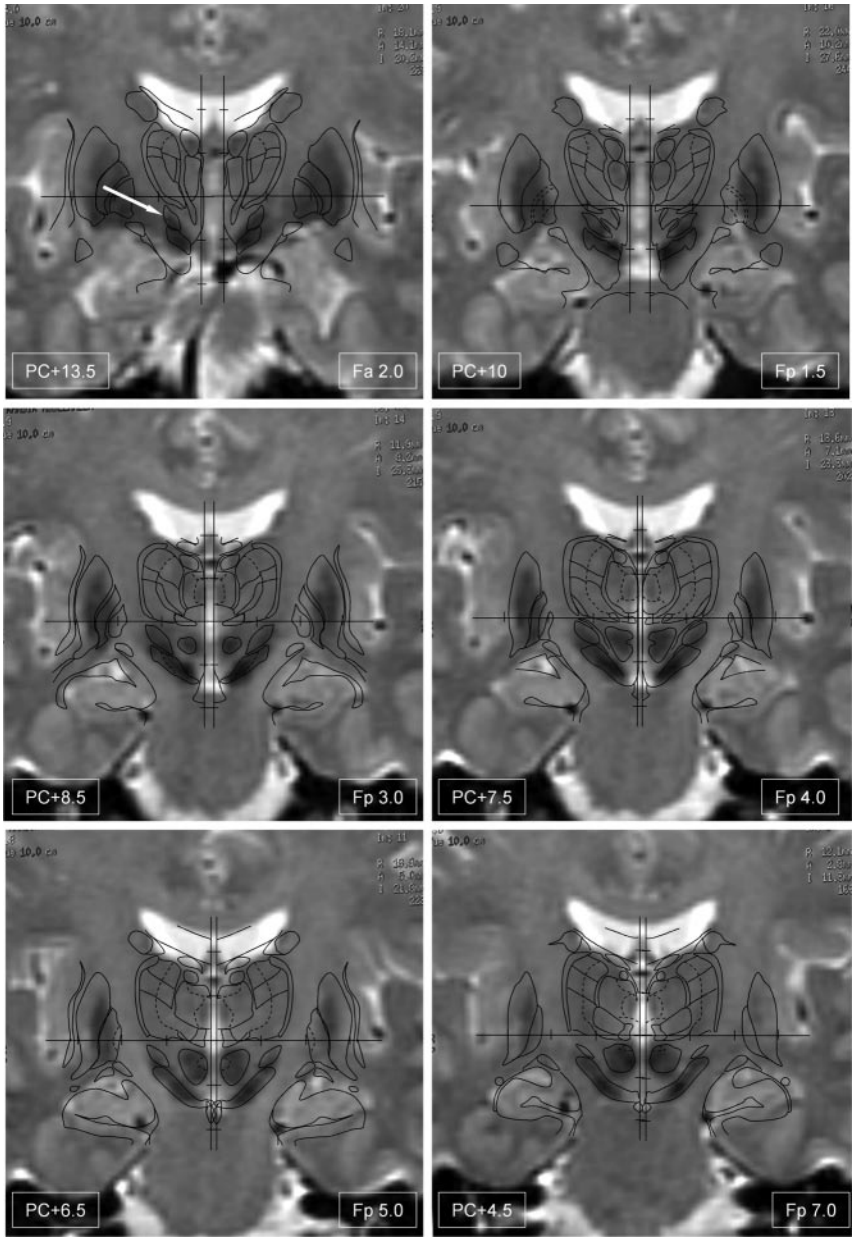

FIG 1. Fusion of the Schaltenbrand and Wahren atlas with the T2-weighted acquisition of a patient with Parkinson's disease. The six anteroposterior levels of the atlas containing a section of the subthalamic nucleus (*arrow* in level Fa 2.0) are represented. Note that the subthalamic nucleus is hypointense at anterior levels (Fa 2.0–Fp 4.0) but only partly hypointense at level Fp 5.0 and not hypointense at the most posterior level (Fp 7.0). The contours of the Schaltenbrand and Wahren atlas are labeled in Figure 3.

crease in the separation between the left and right parts of the Schaltenbrand sections was likely due to the presence of the third ventricle, which was progressively wider in all patients going from its posterior to anterior portion.

In all cases, the STN signal intensity, as evaluated by the two neuroradiologists, presented the same level of hypointensity (mild or prominent) on both sides on the three most anterior sections of the atlas (Fa 2.0, Fp 1.5, and Fp 3.0). On section Fp 4.0, hypointensity was observed in 12 of 15 cases on the left side and in seven of 15 on the right. On section Fp 5.0, hypointensity was observed in six of 15 cases on the left side and in three of 15 on the right. Hypointensity was not observed on either side on the most posterior section (Fp 7.0).

In the anatomic specimen, iron-containing cerebral regions on Perls stained sections were stained blue (Fig 2). The striatum, in particular the putamen, and the external globus pallidus were intensely stained in blue (Fig 2A–C). Perls staining was less visible in the section shown in Figure 2B because neutral red counterstaining was much more intense in that section. Perls staining was also present in the substantia nigra and in the red nucleus (Fig 2D). Within the STN, the Perls reaction was not uniformly intense. It was intense in the anteromedial part of the nucleus (Fig 2A and B) but absent in the dorsolateral part of the STN at the most posterior levels (Fig 2D).

Discussion

Chronic high frequency stimulation of the STN has been shown to be a safe and effective method for treating medically refractory idiopathic Parkinson's disease (4, 6). The STN is shaped like a biconvex lens

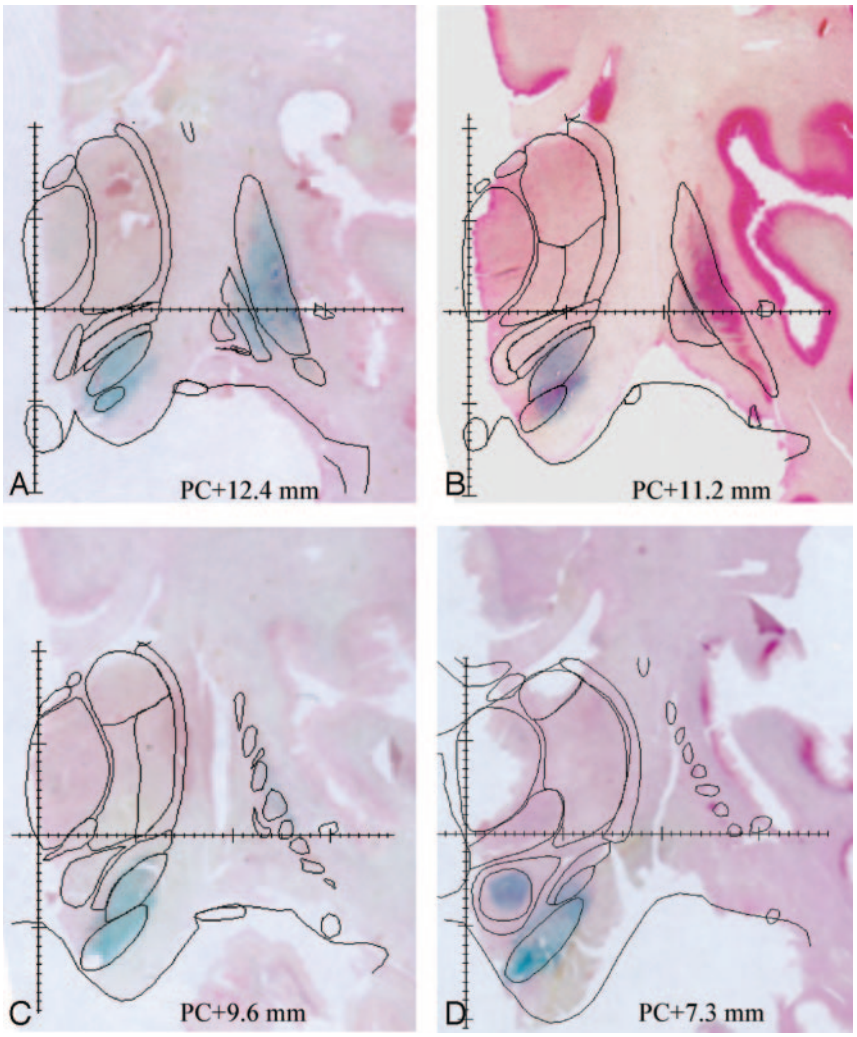

FIG 2. Four sections of an anatomic specimen stained by the Perls method shows the blue stain revealing iron-rich regions. Sections have been counterstained by using neutral red. The contours of cerebral regions have been traced by using the counterstaining of the Perls stained section and Nissl staining of the adjacent sections. Note that the Perls reaction is positive in the anterior portion of the subthalamic nucleus (posterior commissure, +12.4 mm) but very weak in its posterior portion (posterior commissure, +7.3 mm).

and lies ventral to the thalamus, medial to the peduncular portion of the internal capsule, and lateral and caudal to the hypothalamus. Caudally, the medial part of the nucleus overlies the most rostral portions of the substantia nigra (5). The STN is a small nucleus, which, in humans, is estimated to be $3 \times 5 \times 12$ mm (22). It is obliquely oriented on the three anatomic planes. Because of its small size, lenticular shape, and oblique orientation, most centers include peroperative physiological confirmation by using microelectrode recording or semi-microelectrode recording to confirm the exact location of the STN target. It is therefore imperative for the anatomic localization of this nucleus to be as accurate as possible to minimize the number of microelectrode recording trajectories.

Many different anatomic targeting methods have been used to localize the STN. These methods can be classified as direct and indirect. The indirect methods are based on the identification of the anterior and posterior commissure points and the use of human atlases. The coordinates of the anterior and posterior commissure and of the midline sagittal plane can be determined by using CT, MR imaging, or ventriculography (23–26). The direct methods are based on the use of MR images that allow the visualization of the STN. Although some authors have described the use of inversion recovery sequences, the most frequently used sequence for targeting the STN is a T2-weighted sequence (1, 27–29). In this type of sequence, the STN has been identified as a bilateral hypointense signal intensity lateral and dorsal to the substantia nigra (which also appears hypointense), on the frontal section (perpendicular to the anterior commissure-posterior commissure line), located at the level of the anterior limit of the red nucleus (1). However, to our knowledge, no published data have shown that this hypointense zone corresponds to the STN.

MR Signal Intensity of the STN

Our results show that the STN, as defined by using a computerized version of the Schaltenbrand and Wahren atlas, appears as a hypointense structure on heavily T2-weighted sequences. Hypointensity was always observed at the level of the three most anterior sections of the STN (Fp 3, Fp1.5, and Fa 2), which include the two sections of the atlas corresponding to the anterior limit of the red nucleus (Fp 3 and Fp 1.5).

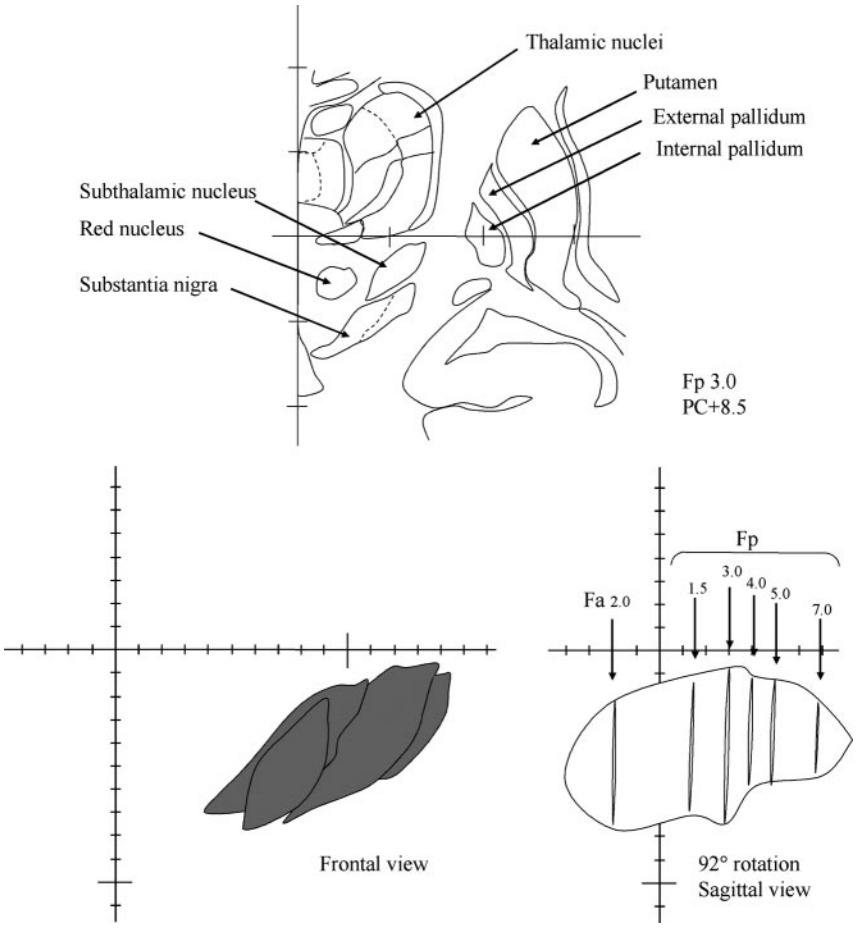

FIG 3. Position of the frontal sections on Schaltenbrand and Wahren atlas along the antero-posterior axis.

Top, Digitized frontal section of the Schaltenbrand and Wahren atlas (Fp 3.0). The main cerebral structures are indicated.

Bottom left, Frontal anterior view of the left subthalamic nucleus obtained by superimposing the six frontal sections of the Schaltenbrand and Wahren atlas containing the subthalamic nucleus.

Bottom right, Sagittal obtained by a 92-degree rotation of the same six frontal contours of the subthalamic nucleus. Note that frontal contours are irregularly spaced from the anterior level Fa 2.0 to the posterior level Fp 7.0, and that there are fewer sections located at the level of the anterior part of the nucleus than at the posterior part.

It must be emphasized that because the frontal sections on the Schaltenbrand and Wahren atlas are irregularly spaced (Fig 3), there are twice as many sections for the posterior half of the STN (Fp 3, Fp4, Fp5, Fp7) as for its anterior half (Fp1.5 and Fa2). However, we can conclude from our data on 15 patients that the anterior half of the STN always appeared hypointense on the T2-weighted sequence used in our study. On section Fp 4, 2.5 mm behind the midportion of the STN (section Fp 3), hypointensity was observed in more than two-thirds of the cases (12 of 15 cases) on the left side and in approximately half of the cases on the right side (seven of 15 cases). More posteriorly, the STN was hypointense in less than half of the cases in section Fp5 and in none of the cases in the most posterior section (Fp7). Thus, the anterior half of the STN was always hypointense, whereas this hypointensity disappeared progressively from anterior to posterior.

Hypointensity at the level of the basal ganglia has been attributed to magnetic susceptibility effects. In our patients, hypointensity at the level of the anterior part of the STN on T2-weighted images was observed on "classical" spin-echo images, as described by Bejjani et al (1). This type of sequence was used because it is very sensitive to magnetic susceptibility effects. Classical spin-echo is more sensitive to magnetic susceptibility effects than is fast spin-echo because it uses a long TE (90 in our sequence), allowing the spins to dephase as they diffuse in regions with different magnetic fields. Fast spin-echo (or turbo spin-echo) sequences use multiple successive echoes (echo train) for each TR by means of rapidly repeated 180-degree pulses; the effective TE is the TE of the echo train that has the weakest value of the phase-encoding gradient, but the real echo spacing is usually in the order of 12 to 20 ms. Thus, the relatively short echo time (echo spacing) leaves little time for the spins to dephase and reduce the sensitivity of these sequences to magnetic susceptibility (30). The parameters of the T2-weighted sequences used are not always clearly indicated in the published reports (6, 27–29, 31), but in most cases, the sequence used is a fast spin-echo sequence. Its sensitivity to magnetic susceptibility and to the hypointensity of the STN nucleus may therefore be less than the sensitivity of a conventional T2-weighted sequence.

Atlas-MR Image Fusion Procedure

The technique that we used to fuse the digitized sections of the Schaltenbrand and Wahren atlas with the MR sections was based on the visualization of anatomic landmarks located near the STN, in particular, the substantia nigra and red nucleus, which are clearly seen as hypointense structures. The lateral wall of the third ventricle and the floor of the lateral ventricles were always easy to identify because of the

high signal intensity of CSF. The software used allowed independent scaling factors to be applied in the dorsoventral (superoinferior) and the mediolateral directions (18). The mean correction factors for the 15 brains were 0.91 and 0.99 in the dorsoventral and mediolateral directions, respectively. This means that the brain used for the frontal sections of the Schaltenbrand and Wahren atlas was globally larger in the dorsoventral direction than the mean of our population, and it was almost the same size as the mean in the mediolateral direction.

A limitation of our study is that we used the Schaltenbrand and Wahren atlas; although it is the most commonly used atlas of the human basal ganglia, as discussed above, it provides relatively few and irregularly spaced sections at the level of the STN. Moreover, the linear transformations of the brain atlas that we used are not necessarily the most appropriate, because they imply the questionable assumption that all structures can be stretched or shrunk by the same factor along a given dimension. Computational mapping of different individual brains onto a single, standardized brain map is a complex and important problem that has not yet been solved (20, 32). However, considering the clear visualization on MR images of the anatomic structures (i.e., substantia nigra, red nucleus, and lateral wall of the third ventricle) used to fuse MR data with atlas data and considering their proximity to the STN, we assume that the determination of the position of the STN was reliable.

Iron Distribution and MR Signal Intensity at the Level of the Basal Ganglia

The STN is one of the nuclei of the basal ganglia, a system that presents a characteristic hypointense signal intensity on T2-weighted images. This property has been attributed to the presence of iron (10). A progressive increase in iron concentration is a unique characteristic of the basal ganglia system (33). It has been shown that T2 hypointensity in specific gray matter regions is absent in young children but becomes progressively prominent as adulthood is approached (15, 34, 35), and that this is one of the most obvious changes in the brain associated with normal aging (11, 15). The most probable explanation remains an increase in iron deposition (15), the decrease in the signal intensity on T2-weighted images being attributed to a T2* effect. Areas of prominent hypointensity on images obtained with a long TR and a long TE in the basal ganglia ("iron-map on T2") correlate closely with the presence of ferric iron, as documented by the Perls Prussian blue reaction in gross specimens (10, 16, 36, 37). The concentration of iron in the basal ganglia of the adult brain has been shown to be highest at the level of the globus pallidus, red nucleus, and substantia nigra, lowest at the level of the thalamus, and intermediate at the level of the putamen and caudate nucleus (33). A similar distribution has been described in the monkey (38). These concentrations are well correlated with the classical hypointense signal intensity observed on T2-weighted images at the level of the pallidum, red nucleus, and substantia nigra in the adult and aging brain. Despite numerous studies of the presence of iron in the basal ganglia of the adult and aging brain, to our knowledge, no studies have been conducted of the iron content in the STN, nor have any descriptions of its aspect by using Perls Prussian blue reaction been reported. It should be noted that although the authors make no reference to it, one of the figures in the article by Rutledge et al (33) clearly shows the presence of a high concentration of iron at the level of the STN revealed by Perls Prussian blue reaction.

Anatomic Iron Distribution at the Level of the STN

The Perls staining that we performed on an anatomic specimen suggests that the hypointense MR signal intensity at the level of the STN can be attributed, as in other nuclei of the basal ganglia system, to the presence of iron. As was the case with the hypointense MR signal intensity, the Perls reaction (i.e., presence of iron) was clearly predominant at the level of the anteromedial half of the STN whereas it was absent at its posterolateral pole. This topography, which suggests that different portions of the STN might contain different densities of iron, could correspond to the different territories identified in the STN of monkeys on the basis of tract tracing studies (39). The STN and other structures of the basal ganglia are considered to comprise three functional territories, referred to as *sensorimotor*, *associative*, and *limbic*, which are thought to process motor, cognitive, and emotional information, respectively. In the STN, the dorsolateral portion corresponds to the sensorimotor territory, whereas the anteromedial pole would correspond to the limbic territory and the intermediate portion to the associative territory (39). The reason the posterior portion of the sensorimotor territory is apparently devoid of iron is not yet known.

Implications for the Stereotactic Treatment of Parkinson's Disease

Our data showed that the hypointense signal intensity on coronal T2-weighted images above and lateral to the substantia nigra corresponded to the STN. This validates the use of T2-weighted images for targeting the STN in stereotactic interventions, as previously described (2). It must be emphasized, however, that only the anterior half of the STN is hypointense in all cases and thus always visible on T2-weighted images. In many cases, the most posterior part of the nucleus is not hypointense and remains invisible on T2-weighted images. Thus, the most posterior part of the sensorimotor STN is not visible on T2-weighted images in most cases. However, on the sections that correspond to the target described by Bejjani et al (1) (Fp3 and Fp1.5 located at the level of the anterior limit of the red nucleus), the STN was always hypointense. This result once again validates the use of this targeting method and shows that the T2 target corre-

sponds to the anterior half of the nucleus. Because the sensorimotor part of the STN represents by far the largest part of the nucleus, the T2 target clearly corresponds to a sensorimotor portion of the STN. However, as the anteromedial associative-limbic part of the nucleus is also always hypointense, its exact limit with the sensorimotor portion cannot be clearly determined.

The MR acquisitions that we used in our study were obtained from a population of patients with advanced Parkinson's disease selected for stereotactic surgery at the level of the STN. Our results can thus be used to target the STN in the same type of patients with advanced Parkinson's disease. Conversely, our anatomic data were obtained from the brain of a study participant who did not have neurologic disease. Yet, because the pattern of iron distribution at the level of the STN (Perls staining in the nucleus except at its most posterior part) closely corresponded to the T2 hyposignal in our patients, it is legitimate to conclude that at the level of the STN, the distribution of iron is correlated with the T2 hyposignal. Some authors have described an increase in iron content in the substantia nigra pars compacta, the putamen, and the pallidum of patients with Parkinson's disease (14, 40). The causes of this phenomenon are still under investigation (14, 41) and may reflect some nonspecific effect of degeneration (42). To our knowledge, no data in the literature concerning a modification of iron content at the level of the STN in Parkinson's disease have been reported, and it is not possible to determine whether such modification exists, based on our data. A study of a large population of healthy volunteers of various ages would be necessary to determine whether any modification of iron concentration occurs with age at the level of the STN and whether iron distribution in the STN is modified in Parkinson's disease.

Conclusion

To our knowledge, our study is the first to show that the hypointense signal intensity located lateral to the red nucleus and dorsolateral to the substantia nigra corresponds anatomically to the STN and thus can be used as a landmark for electrode implantation at the level of the STN in patients with Parkinson's disease. MR hypointensity at the level of the STN is due to the presence of iron, as shown on an anatomic specimen by using Perls staining. It should be stressed, however, that although hypointensity was present in the anterior half of the STN in all patients with Parkinson's disease, the posterior part of the nucleus was not visible in most cases.

References

1. Bejjani BP, Dormont D, Pidoux B, et al. **Bilateral subthalamic stimulation for Parkinson disease by using three-dimensional stereotactic magnetic resonance imaging and electrophysiological guidance**. *J Neurosurg* 2000;92:615–625
2. Voges J, Volkmann J, Allert N, et al. **Bilateral high-frequency stimulation in the subthalamic nucleus for the treatment of Parkinson disease: correlation of therapeutic effect with anatomical electrode position**. *J Neurosurg* 2002;96:269–279
3. Pollak P, Benabid AL, Limousin P, Benazzouz A. **Chronic intracerebral stimulation in Parkinson's disease**. *Adv Neurol* 1997;74:213–220
4. Limousin P, Pollak P, Benazzouz A, et al. **Effect of parkinsonian signs and symptoms of bilateral subthalamic nucleus stimulation**. *Lancet* 1995;345:91–95
5. Carpenter M. **The subthalamic region**. In: Carpenter M, ed. *Human Neuroanatomy.* Baltimore: Williams & Wilkins; 1976:509–511
6. Zonenshayn M, Rezai AR, Mogilner AY, Beric A, Sterio D, Kelly PJ. **Comparison of anatomic and neurophysiological methods for subthalamic nucleus targeting**. *Neurosurgery* 2000;47:282–294
7. Schuurman PR, de Bie RM, Majoie CB, Speelman JD, Bosch DA. **A prospective comparison between three-dimensional magnetic resonance imaging and ventriculography for target-coordinate determination in frame-based functional stereotactic neurosurgery**. *J Neurosurg* 1999;91:911–914
8. Starr PA, Vitek JL, DeLong M, Bakay RA. **Magnetic resonance imaging-based stereotactic localization of the globus pallidus and subthalamic nucleus**. *Neurosurgery* 1999;44:303–314
9. Benabid AL, Benazzouz A, Gao D, et al. **Chronic electrical stimulation of the ventralis intermedius nucleus and of other nuclei as a treatment for Parkinson's disease.** *Tech Neurosurg* 1999;5:5–30
10. Drayer B, Burger P, Darwin R, Riederer S, Herfkens R, Johnson GA. **MRI of brain iron**. *AJR Am J Roentgenol* 1986;147:103–110
11. Drayer BP. **Imaging of the aging brain: part I: normal findings**. *Radiology* 1988;166:785–796
12. Thomas LO, Boyko OB, Anthony DC, Burger PC. **MR detection of brain iron**. *AJNR Am J Neuroradiol* 1993;14:1043–1048
13. Ordidge RJ, Gorell JM, Deniau JC, Knight RA, Helpern JA. **Assessment of relative brain iron concentrations using T2-weighted and T2*-weighted MRI at 3 Tesla**. *Magn Reson Med* 1994;32:335–341
14. Ye FQ, Allen PS, Martin WR. **Basal ganglia iron content in Parkinson's disease measured with magnetic resonance**. *Mov Disord* 1996;11:243–249
15. Drayer BP. **Basal ganglia: significance of signal hypointensity on T2-weighted MR images**. *Radiology* 1989;173:311–312
16. Chen JC, Hardy PA, Kucharczyk W, et al. **MR of human postmortem brain tissue: correlative study between T2 and assays of iron and ferritin in Parkinson and Huntington disease**. *AJNR Am J Neuroradiol* 1993;14:275–281
17. Gomori JM, Grossman RI. **The relation between regional brain iron and T2 shortening**. *AJNR Am J Neuroradiol* 1993;14:1049–1050
18. Yelnik J, Damier P, Demeret S, et al. **Localization of stimulating electrodes in patients with Parkinson's disease by using a three-dimensional atlas-magnetic resonance imaging coregistration method**. *J Neurosurg* 2003;99:89–99
19. Schaltenbrand G, Wahren W. *Atlas for Stereotaxy of the Human Brain*. Georg Thieme Verlag, 1977
20. Yelnik J, Damier P, Bejjani BP, et al. **Functional mapping of the human globus pallidus: contrasting effect of stimulation in the internal and external pallidum in Parkinson's disease**. *Neuroscience* 2000;101:77–87
21. Perls M. **Evidence for the presence of iron oxide in certain pigments [in German].** *Virchows Arch Path Anat* 1867;39:42–48
22. Yelnik J. **Functional anatomy of the basal ganglia [Suppl 3].** *Mov Disord* 2002;17:S15–S21
23. Hariz MI, Bergenheim AT. **A comparative study on ventriculographic and computerized tomography-guided determinations of brain targets in functional stereotaxis**. *J Neurosurg* 1990;73:565–571
24. Holtzheimer PE III, Roberts DW, Darcey TM. **Magnetic resonance imaging versus computed tomography for target localization in functional stereotactic neurosurgery**. *Neurosurgery* 1999;45:290–298
25. Laitinen LV, Bergenheim AT, Hariz MI. **Leksell's posteroventral pallidotomy in the treatment of Parkinson's disease**. *J Neurosurg* 1992;76:53–61
26. Tasker RR, Dostrovsky JO, Dolan EJ. **Computerized tomography (CT) is just as accurate as ventriculography for functional stereotactic thalamotomy**. *Stereotact Funct Neurosurg* 1991;57:157–166
27. Patel NK, Heywood P, O'Sullivan K, Love S, Gill SS. **MRI-directed subthalamic nucleus surgery for Parkinson's disease**. *Stereotact Funct Neurosurg* 2002;78:132–145
28. Egidi M, Rampini P, Locatelli M, et al. **Visualisation of the subthalamic nucleus: a multiple sequential image fusion (MuSIF) technique for direct stereotaxic localisation and postoperative control [Suppl 2].** *Neurol Sci* 2002;23:S71–S72
29. Saint-Cyr JA, Hoque T, Pereira LC, et al. **Localization of clinically effective stimulating electrodes in the human subthalamic nucleus on magnetic resonance imaging**. *J Neurosurg* 2002;97:1152–1166
30. Bradley WG, Chen DY, Atkinson DJ, Edelman RE. **Fast spin-echo**

and echo-planar imaging. In: Bradley WG, ed. *Magnetic Resonance Imaging.* St Louis: Mosby; 1999:125–157
31. Benabid AL, Koudsie A, Benazzouz A, Le Bas JF, Pollak P. **Imaging of subthalamic nucleus and ventralis intermedius of the thalamus [Suppl 3].** *Mov Disord* 2002;17:S123−S129
32. Starr PA, Christine CW, Theodosopoulos PV, et al. **Implantation of deep brain stimulators into the subthalamic nucleus: technical approach and magnetic resonance imaging-verified lead locations**. *J Neurosurg* 2002;97:370–387
33. Rutledge JN, Hilal SK, Silver AJ, Defendini R, Fahn S. **Study of movement disorders and brain iron by MR**. *AJR Am J Roentgenol* 1987;149:365–379
34. Aoki S, Okada Y, Nishimura K, et al. **Normal deposition of brain iron in childhood and adolescence: MR imaging at 1.5 T**. *Radiology* 1989;172:381–385
35. Hallgren B, Sourander P. **The effect of age on the non-haemin iron in the human brain.** *J Neurochem* 1958;3:41–51
36. Milton WJ, Atlas SW, Lexa FJ, Mozley PD, Gur RE. **Deep gray matter hypointensity patterns with aging in healthy adults: MR imaging at 1.5 T**. *Radiology* 1991;181:715–719
37. Pujol J, Junque C, Vendrell P, et al. **Biological significance of iron-related magnetic resonance imaging changes in the brain**. *Arch Neurol* 1992;49:711–717
38. Francois C, Nguyen-Legros J, Percheron G. **Topographical and cytological localization of iron in rat and monkey brains**. *Brain Res* 1981;215:317–322
39. Parent A. **Extrinsic connections of the basal ganglia**. *Trends Neurosci* 1990;13:254–258
40. Riederer P, Dirr A, Goetz M, Sofic E, Jellinger K, Youdim MB. **Distribution of iron in different brain regions and subcellular compartments in Parkinson's disease [Suppl].** *Ann Neurol* 1992;32:S101−S104
41. Dexter DT, Jenner P, Schapira AH, Marsden CD. **Alterations in levels of iron, ferritin, and other trace metals in neurodegenerative diseases affecting the basal ganglia: The Royal Kings and Queens Parkinson's Disease Research Group**. *Ann Neurol* 1992;32[suppl]:S94−S100
42. Dexter DT, Carayon A, Javoy-Agid F, et al. **Alterations in the levels of iron, ferritin and other trace metals in Parkinson's disease and other neurodegenerative diseases affecting the basal ganglia**. *Brain* 1991;114:1953–1975